Analyst

Accepted Manuscript

ROYAL SOCIETY OF CHEMISTRY

www.rsc.org/analyst

Analysis of the developing neural system using an in vitro model by Raman spectroscopy

Kosuke Hashimoto[1], Suguru N. Kudoh[2], and Hidetoshi Sato[1*]

[1]Department of Bioscience and [2]Department of Human System Interaction

School of Science and Technology, Kwansei Gakuin University

2-1, Gakuen, Sanda, Hyogo 669-1337 Japan.

*Corresponding author,

Phone & Fax: +81-79-565-7228; E-mail address: hidesato@kwansei.ac.jp

Abstract

We developed an in vitro model of early neural cell development. The maturation of a normal neural cell was studied in vitro using Raman spectroscopy for 120 days. The Raman spectra datasets were analyzed by principal component analysis (PCA) to investigate the relationship between maturation stages and molecular composition changes in neural cells. According to the PCA, the Raman spectra datasets can be classified into four larger groups. Previous electrophysiological studies have suggested that a normal neural cell goes through three maturation states. The groups we observed by Raman analysis showed good agreement with the electrophysiological results, except with the addition of a fourth state. The results demonstrated that Raman analysis was powerful to investigate the daily changes in molecular composition of the growing neural cell. This in vitro model system may be useful for future studies of the effects of endocrine disrupters in the developing early neural system.

1. Introduction

It is important to study the functions of the neural cell (neuron) in order to understand mental activity and the neural system as a whole. Knowledge of neural systems may allow for the development of new therapeutic techniques for neurological diseases such as dementia and Parkinson's disease. In the present study, we employ an optical technique, Raman spectroscopy, instead of electrophysiological methods to investigate the relationship between molecular alterations and electrical activity in live growing neural cells in vitro. The central nervous system is mainly composed of five types of cells: neurons, oligodendrocytes, microglia, astrocytes, and ependymal cells. Although neurons are small in number of all cells, they are responsible for the essential functions of the brain, such as physical and emotional activities. The other cells, collectively called glia, provide support to the neural cells. Neurons are always active, and generate electrical pulses even in the absence of external stimulation or during sleep.[1] This spontaneous neural firing is even observed in visual nerve cells of mouse embryos, although the cells have never been exposed to light.[2] Initially, this spontaneous firing was thought to be merely noise. However, Ikegaya et al. observed synchronized spontaneous firings of neocortical neurons in a live brain slice using a calcium imaging technique.[3] Kiyohara et al. used electrophysiology to investigate the relationships between evoked and spontaneous activity in a mature nerve cell model system cultured in a dish.[4] The nerve cells in the model system were collected from the hippocampus of a rat fetus. The researchers cultured the neural cells in a dish with multichannel electrodes, and observed the electrical properties of the live growing cells for around 80 days. The cells were silent for the first several days in vitro (DIV). Random electrical pulses were observed at 10 DIV, which were due to the unorganized spontaneous firing of the neural cells. After 60 DIV, synchronized "burst" signaling activity was observed, which suggested that the cells in the

culture dish had formed a network. These results indicate that the neural cell undergoes at least three maturation states during the organization of an integrated system in the dish. The cell has an independent state initially, following its differentiation from a neural stem cell. The cell gains the ability to fire electrical pulses randomly in the second state, and it begins making physical contacts with neighboring neural cells. In the third state, all cells in the dish have a greater degree of interaction with each other and are organized into one system. In this state, an electrical signal is efficiently transferred between cells resulting in a synchronized signal burst.

In the field of developmental psychology, researchers have recently begun to pay significant attention to endocrine disrupters. Some researchers have reported the effects of one particular endocrine disrupter, bisphenol A (BPA), on the behavior of children. BPA is an additive agent for plastics such as polycarbonate and epoxy resins. It has a structure similar to estrogen, and is able to bind to the estrogen receptor and disturbs estrogenic signaling pathways.[5] Zoeller et al. reported that BPA can also bind to the rat thyroid hormone (TH) receptor and act as an antagonist of TH, which is an essential hormone for normal brain development.[6] Further, Ishido et al. reported that 5-day-old rats exposed to 0.2-20 μg of BPA showed the typical symptoms of attention deficit hyperactivity disorder (ADHD).[7] These reports have emphasized the importance of studying the effects of endocrine disrupters on young neural cells in the early stages of brain development.

The purpose of the present study was to establish an in vitro model system that mimics the early stages of neural development, and to propose a method to monitor the response and maturation of cells by Raman analysis. Raman spectroscopy is a powerful technique to analyze live cells in vitro. For example, Oshima et al. successfully discriminated between four cancer cells and one normal cell by Raman spectroscopy without any sample treatments. In

that study, principal component analysis (PCA) was used to discriminate the data groups.[8] Ghita et al. used Raman spectroscopy as a noninvasive, label-free technique to identify, image, and quantify potential molecular markers of neural stem cell differentiation status in vitro.[9] Raman spectroscopy is also very powerful for long term observation because it is very low or no invasive to the live cells.[10,11] Using live giant squid axons, Nagashima et al. detected the unique coherent anti-Stokes Raman scattering (CARS) spectra of sevoflurane.[12] Ajito et al. employed a laser trapping technique with Raman analysis to observe the exocytosis of glutamic acid in a synaptosome isolated from a live neural cell.[13] The utility of Raman analysis for detection of viral infection in live cells has also been reported.[14] These previous reports reveal that multivariate analysis based on Raman spectroscopy is highly sensitive to any cellular changes due to external perturbations.

In the present study, we developed an in vitro neural development model system and analyzed its normal changes during the process of maturation. Animal models are not optimal for studying the effects of endocrine disrupters, because the in vivo neural system is highly complex and the small size of the mouse fetus makes experimental procedures difficult. Moreover, the cost and time for each experiment is substantial, because it is necessary to sacrifice an animal at every time point for measurements. In contrast, studying an in vitro model system with Raman analysis is simple and less costly. In this system, the researcher can observe the state of cells repeatedly by Raman analysis without causing any cellular damage. Neural cells undergo significant changes during the stages of maturation, and it is important to collect basic data regarding the normal maturation states of cultured cells. In the future, the present Raman analytical method and basic knowledge of cell maturation states can be extended to 3D cultured nerve systems and/or live brain slice models with new Raman imaging technologies.[15-18]

2. Materials and Methods

2. 1 Primary culture of rat hippocampal neural cells

The hippocampus was dissected from the brains of Wistar rats (CLEA Japan, Inc., Tokyo, Japan) at embryonic day 18. The dura mater and other surrounding tissues were carefully removed, and the hippocampus was washed three times with Ca^{2+} and Mg^{2+} free phosphate buffered saline (PBS(-), Life Technologies, NY, USA). This procedure eliminated potential fibroblast contamination from the dura mater and other surrounding tissues. Hippocampal neurons were dissociated into single cells by treating them with 0.125% trypsin-EDTA (Wako Pure Chemical Industries, Ltd., Osaka, Japan) in PBS(-) at 37°C for 10 min. The cells were rinsed with PBS(-) three times and transferred into 2 mL of culture medium. The culture medium consisted of Neurobasal A medium (Life Technologies) with 0.5 mM L-glutamine, B27 supplement, and 100 Units/mL of penicillin-streptomycin. The cell density was 100,000 cells/mL. The suspension was transferred into a 35-mm polyethyleneimine-coated dish with a quartz window at the bottom (Fine Plus International, Ltd., Kyoto, Japan). Ten dishes of sample were prepared from about 10 embryos obtained from one rat. The cells were cultured in an incubator at 37°C with 5% CO_2 and saturated humidity. Half of the culturing medium was changed every 3 days. The Raman measurements were carried out at 2, 8, 15, 30, 45, 60, 75, 90, 105, and 120 days after the cell seeding. The sample was discarded after every measurement because there was possibility of contamination during the measurement. This study was approved by the ethics committee of Kwansei Gakuin University.

2. 2 Immunostaining

Immunostaining was carried out for the microscopic observation of neural cells. The cells

were cultured for 120 days, and were stained following the Raman measurement. The cells were washed twice in PBS(-), then fixed with methanol (Wako Pure Chemical Industries, Ltd.) at -20°C for 10 min. The methanol was washed out by soaking the sample in PBS(-) three times for 5 min each time. The fixed cells were treated with TritonX-PBS (0.2%) for 1 min to permeabilize the membranes, then blocked with goat serum (10%) at 37°C for 1 h. The sample was treated with rabbit polyclonal MAP2 antibody (1:1000; EMD Millipore, MA, USA) and mouse IgG1 monoclonal GFAP antibody (3 μg/mL; Sigma-Aldrich, MO, USA) at 37°C for 2 h. After treatment with the primary antibodies, the sample was washed with PBS(-) three times for 5 min each. The secondary antibodies were Alexa Fluor® 546 conjugated anti-rabbit IgG and Alexa Fluor® 647 conjugated anti-mouse IgG1 (Life Technologies), and treatment was conducted in the dark for 1 h at room temperature. The cell nuclei were stained with 4',6-diamidino-2-phenylindole (DAPI; SouthernBiotech, AL, USA). Fluorescent images were observed with an A1 confocal fluorescence microscope (Nikon, Tokyo, Japan).

2. 3 Raman analysis

Raman spectra were measured with a confocal micro-Raman system (Nanofinder30, Tokyo Instruments Inc., Tokyo, Japan) with a CO_2 incubating sample holder as shown in Fig. 1. The system was equipped with a 600 lines/mm grating (blazed at 750 nm), CCD cooled to -80°C (DU420-BRDD; Andor Technology Co. Ltd., Northern Ireland), and continuous-wave background-less electrically tuned Ti:Sapphire laser (CW-BL-ETL) which provided excitation light at 785 nm.[19] The excitation laser was focused by a 60× water immersion objective lens (N.A. 1.1, LUMFLN; Olympus, Tokyo, Japan). The power was typically 35 mW at the sampling point. The lateral and vertical spatial resolutions were estimated to be 1 and 5 μm, respectively. The Raman measurement acquisition time was 90 s. The Raman scattered light

was collected at the back scattered configuration. The background spectra of quartz and culture medium were subtracted from the spectra. Further background correction was carried out by subtracting the 11th-order polynomial-fitted background to remove baseline undulation. Spectra were normalized with a standard band at 1450 cm^{-1}, which is assigned to the CH_2 deformation mode,[20] prior to the multivariate analysis. The Raman spectra were analyzed with The Unscrambler multivariate analysis software (Camo, Oslo, Norway).

3. Results and Discussion

3. 1 Morphological observation of cell growth

For the Raman measurement, an area of cultured cells with a suitable density was selected. Bright field images of cultured neural cells at 2, 15, 60, and 90 DIV are shown in Fig. 2 (a)-(d). There were neuronal and glial cells in the dish, and no fibroblasts were observed in the 2 DIV image (a). The neural cell (solid arrow) has a well-defined nucleus and looks sharp. In contrast, the glial cell (dotted arrow) shows flat stubby feature and no defined nucleus. At this point, the neural cell was in the G0 state and ceased to proliferate.[21] The cell body, axon, and dendrites grew considerably from 2 to 15 DIV, but the cell density in the dish was still relatively low. At 60 and 90 DIV, the neural cells further extended their axon and dendrites to construct a network. There was a higher density of both glia and neural cells, such that their cell bodies overlapped. No fibroblasts were seen in the culture. Considering fibroblasts proliferate quickly, within 10 days they would occupy most of the space in the dish when seeded with G0 phase neurons. Thus, their absence suggests that the sample preparation procedure was effective. Glial cells have features similar to those of neural cells, but lack an axon. Since it is necessary to visually select a neural cell for the Raman measurement, the cell density should not be too high. However, the neural cell needs to have intercellular

connections to correctly build a network. We investigated the optimal cultured cell density for Raman observation. In the present study, the initial cell density seeded into the dish was approximately 250 cells/mm^2.

Pseudo-colored immunostained images of the neural cell at 120 DIV are shown in Fig. 2 (e). The cells were stained with antibodies to MAP2 and GFAP. The MAP2 (green) protein exists in the neural cell body and dendrites and GFAP (red) is found in the cell body of the astrocyte. The nucleus was stained with DAPI (blue). The axon of the neural cell was not visible in the image because it lacks MAP2. The cell bodies of oligodendrocytes and microglial cells were also not observed because they lack GFAP. Neural cells have a larger nucleus than glia, and the neural cell body is surrounded astrocytes, which regulate synaptic transmission and supply energy to these cells.[22] Some isolated blue spots may represent the nuclei of oligodendrocytes, which form the myelin sheath around the axon, and microglia, which act as immune cell-like scavengers in the brain.

3. 2 Raman analysis

Raman spectra were collected only from the neural cells. It was easy to discriminate the neural cells from the glial cells by visual selection in bright field images as shown in Fig. 2. We focused the laser on the nucleus, cytoplasm, and dendrites to measure and compare the respective spectra (data not shown). Results indicated that the nuclear spectra were of much higher quality than the spectra of the cytoplasm and dendrites. Hence, the nuclear spectra were used for analysis in this study. Averaged Raman spectra of cells cultured for 2, 8, 15, 30, 45, 60, 75, 90, 105, and 120 DIV are shown in Fig. 3 (a)-(j).The intensity of the spectra were normalized with the standard band at 1450 cm^{-1}, which is assigned to the CH_2 and CH_3 bending modes. This reflects the amount of CH bonding in all organic materials in the cell. A

band at 785 $cm^{-1}$was assigned to DNA, which was observed most strongly in the 2 DIV spectrum. Bands at 1663 and 1339 cm^{-1} were assigned to amide I and amide III modes of proteins. A band at 1251 cm^{-1} arose from the amide III mode of proteins and the C=CH mode of lipids. The intensity of the band reflects the concentration of material included in the excitation volume of the focal point. The neural cell did not proliferate in the present culturing condition, meaning no duplication of DNA had taken place. As observed in the microscopic image, the size of the nucleus was smallest at 2 DIV compared to the other culturing days. This indicates that the DNA density was highest in the neural cell at 2 DIV, because the total molecular weight of DNA was static. According to the subtraction (data not shown), the bands at 1093 and 1003 cm^{-1} showed a reduced intensity when the cells were cultured longer. They arose from phenylalanine and DNA, respectively. As the neural cell does not proliferate and the cell cycle is arrested at G0,[21] these molecular changes were attributed to the growth of the neural cell. A spectrum (k) in Fig. 3 is the averaged spectrum of cytoplasm. The band at 785 cm^{-1} due to DNA is missing. As it has lower signal-to-noise ratio, we did not use the spectra of cytoplasm in the detailed analysis.

PCA was applied to analyze the results in more detail. PCA score plots for PC1, 2, and 3 are depicted in Fig. 4. The datasets for the 10 groups of different cell culture DIV lengths are exhibited in the plots. It should be noted that data in this PCA includes the spectra obtained in the three totally independent experiments. There is no clear segmentation observed within each dataset. It suggests high reproducibility and reliability of the present results. The analysis showed that there were four main data groups: (α) 2 DIV, (β) 8-30 DIV, (γ) 45-105 DIV, and (δ) 120 DIV. The α group consisted of the youngest cells and showed good separation from the β group, suggesting that the young neural cells undergo large changes at the beginning of their maturation process. This group represents the earliest stage of the neural cell after its

differentiation from the neural stem cell. In this stage, the cell has no electrical activity, and its axon and dendrites grow quickly. The β group appears to be a transient state. The datasets from different cultivation days were dispersed within this group, but were independent from the other data groups. This group may correspond to the second stage of the neural cell maturation. During this stage, the neural cell shows spontaneous and random firing of electrical pulses. According to the previous electrophysiological study,[4] this stage generally lasts from 10 to 60 DIV. Our Raman analysis detected the transition from the first stage to the second stage slightly earlier than that seen in the electrophysiological observations. Cells belonging to the γ group are relatively stable, because the datasets from different cultivation days overlap with each other in the score plots. Neural cells cultured in vitro generally show synchronized signal burst firing after 60 DIV according to electrophysiological observations, and the present Raman observations are in accordance. The last group, δ, consists only of the dataset from 120 DIV. This group is clearly isolated from the other groups, particularly in PC3 and does not have a corresponding state observed in the electrophysiological study.

The loading plots of PC1 (a), PC2 (b), and PC3 (c) are shown in Fig. 5. The datasets for 2 and 8 DIV have a relatively higher value in PC1 in the score plots (Fig. 4). The PC1 loading plot had strong bands at 788, 1095, 1487 and 1576 cm^{-1}, which were assigned to DNA. This revealed that PC1 reflects the concentration of DNA in the nucleus, because young cells have a relatively smaller nucleus. In contrast, the groups γ and δ had a relatively high value on the PC2 axis. The PC2 loading plot showed slightly more complicated features, and there were small bands in the plot that were difficult to assign. The bands assigned to phenylalanine appeared strongly at 1003 and 1031 cm^{-1}, suggesting that protein species expression differed in mature and young cells. The PC3 axis seemed to reflect the maturation of the neural cells, except for the dataset of 2 DIV. A band at 893 cm^{-1} may be assigned to the C-C skeletal mode

of lipids. Negative features at 1664, 1307 and 1260 cm^{-1} are assignable to C=C stretching, CH_3/CH_2 twisting or bending mode, and C=C-H bending modes of fatty acid chains in lipids. Positive bands at 1441 and 1414 cm^{-1}were thought to reflect structural changes to the backbone to which the CH_2 and CH_3 groups belong. The band at 1330 cm^{-1} was attributed to phospholipids.[23] In summary, these results suggested that compositional changes in lipids take place during the neural cell maturation process. The neural cell initially accelerates growth to extend its axon and dendrites after settling on the dish, and its growth gradually slows down along with the organization of neural system. The cell may need to have a more flexible cytoplasmic membrane with a specific composition of phospholipids during the active maturation phase. Each neighboring two datasets of different culturing date were analyzed with partial least square regression (PLSR).[24,25] The factors to discriminate two groups were mostly admixture of PC1, 2 and 3 in Fig. 5. The only factor between 105 and 120 DIV (data not shown) was not similar to any of them, suggesting that the neural cell makes a characteristic alteration in the δ stage. However, the function and/or character of the cell in this stage is totally unknown at present.

4. Conclusion

The spectral changes of a live growing neural cell were successfully analyzed in the present study. The datasets were classified into 4 groups that reflect the maturation states of the neural cell. The first group consists of the 2 DIV dataset, in which the neural cell has a small nucleus with condensed DNA. The 2 DIV neural cell generally does not show any electrical activity. The second group includes the 8-30 DIV datasets. At this stage, the cell grows actively and has a slightly different composition of lipid species. This group seems to correspond to the maturation stage of random spontaneous signaling. The third group consists

of the 60-90 DIV datasets. The cells in this state showed very similar Raman spectra, indicating that their molecular composition was stable. The fourth group consists of only the 120 DIV dataset. According to the PCA, the lipid composition of the cell at 120 DIV was more similar to that of the cell at 2 DIV. Electrophysiological studies suggest that the neural cells organize into a large system and show signal bursts in the third and fourth groups. Our results indicate that Raman spectroscopy is a powerful noninvasive tool to analyze the maturation stages of neural cells. This method provides information on the molecular composition of live cells without any staining or labeling. In the present study, we succeeded in generating a model dataset that mimics the normal growth of developing neural cells. The response of developing neural cells to endocrine disrupters can be analyzed by a comparison with this model.

References

1. D. A. McCormick, *Science*, 1999, **285**, 541-543.
2. M. Weliky and L. C. Katz, *Science*, 1999, **285**, 599-604.
3. Y. Ikegaya, G. Aaron, R. Cossart, D. Aronov, I. Lampl, D. Ferster and R. Yuste, *Science*, 2004, **304**, 559-564.
4. A. Kiyohara, T. Taguchi and s. N. Kudoh, *The transactions of the Institute of Electrical Engineers of Japan. C, A publication of Electronics, Information and System Society*, 2009, **129**, 1815-1821.
5. N. Ben-Jonathan and R. Steinmetz, *Trends in Endocrinology and Metabolism*, 1998, **9**, 124-128.
6. R. Zoeller, A. Dowling, C. Herzig, E. Iannacone, K. Gauger and R. Bansal, *Environmental Health Perspectives*, 2002, **110**, 355-361.
7. M. Ishido, Y. Masuo, M. Kunimoto, S. Oka and M. Morita, *Journal of Neuroscience Research*, 2004, **76**, 423-433.
8. Y. Oshima, H. Shinzawa, T. Takenaka, C. Furihata and H. Sato, *Journal of Biomedical Optics*, 2010, **15**.
9. A. Ghita, F. Pascut, M. Mather, V. Sottile and I. Notingher, *Analytical Chemistry*, 2012, **84**, 3155-3162.
10. A. Ghita, F. C. Pascut, V. Sottile and I. Notingher, *Analyst*, 2014, **139**, 55-58.
11. F. C. Pascut, S. Kalra, V. George, N. Welcha, C. Denning and I. Notingher, *Biochim. Biophys. Acta*, 2013, **1830**, 3517–3524.
12. Y. Nagashima, T. Suzuki, S. Terada, S. Tsuji and K. Misawa, *Journal of Chemical Physics*, 2011, **134**.
13. K. Ajito, C. Han and K. Torimitsu, *Analytical Chemistry*, 2004, **76**, 2506-2510.

14. K. Moor, K. Ohtani, D. Myrzakozha, O. Zhanserkenova, B. Andriana and H. Sato, *Journal of Biomedical Optics*, 2014, **19**.

15. Y. Oshima, C. Furihata and H. Sato, *Applied Spectroscopy*, 2009, **63**, 1115-1120.

16. Y. Oshima, H. Sato, H. Kajiura-Kobayashi, T. Kimura, K. Naruse and S. Nonaka, *Optics Express*, 2012, **20**, 16195-16204.

17. K. Shi, P. Edwards, J. Hu, Q. Xu, Y. Wang, D. Psaltis and Z. Liu, *Biomedical Optics Express*, 2012, **3**, 1744-1749.

18. A. Silve, N. Dorval, T. Schmid, L. Mir and B. Attal-Tretout, *Journal of Raman Spectroscopy*, 2012, **43**, 644-650.

19. H. Sato, S. Wada and H. Tashiro, *Applied Spectroscopy*, 2002, **56**, 1303-1307.

20. Z. Movasaghi, S. Rehman and I. Rehman, *Applied Spectroscopy Reviews*, 2007, **42**, 493-541.

21. E. Lee, N. Hu, S. Yuan, L. Cox, A. Bradley, W. Lee and K. Herrup, *Genes & Development*, 1994, **8**, 2008-2021.

22. P. Magistretti, L. Pellerin, D. Rothman and R. Shulman, *Science*, 1999, **283**, 496-497.

23. R. Malini, K. Venkatakrishna, J. Kurien, K. Pai, L. Rao, V. Kartha and C. Krishna, *Biopolymers*, 2006, **81**, 179-193.

24. J. Trevisan, J. Park, P. P. Angelov, A. A. Ahmadzai, K. Gajjar, A. D. Scott, P. L. Carmichael and F. L. Martin, *J. Biophotonics*, 2014, **7**, 254-265.

25. M. J. Walsh, A. Hammiche, T. G. Fellous, J. M. Nicholson, M. Cotte, J. Susini, N. J. Fullwood, P. L. Martin-Hirsch, M. R. Alison and F. L. Martin, *Stem Cell Research*, 2009, **3**, 15-27.

Figure Captions

Fig. 1 Scheme of the confocal Raman microscope system equipped with a CO_2 incubator.

Fig. 2 Bright field images of the cultured neural cells at 2 days in vitro (DIV) (a), 15 DIV (b), 60 DIV (c),and 90 DIV (d). A fluorescent image of immunostained neural cells at 120 DIV is shown in (e). Cells were stained with MAP2 (green), GFAP (red) and DAPI (blue).The scale bars in (a) and (e) indicate 50 μm. The solid arrow and dotted arrow in image (a) point at neural and glia cells, respectively.

Fig. 3 Averaged spectra of the neural cells measured at 2 days in vitro (DIV) (a),8DIV (b), 15 DIV (c), 30 DIV (d), 45 DIV (e), 60 DIV (f), 75 DIV (g), 90 DIV (h), 105 DIV (i), 120 DIV (j), and 2 DIV from cytoplasm (k).

Fig. 4 Principal component analysis (PCA) score plots of the datasets for PC1 vs. PC2 (a), PC2 vs. PC3 (b), and PC1 vs. PC3 (c).

Fig. 5 PCA loading plots of PC1 (a), PC2 (b), and PC3 (c).

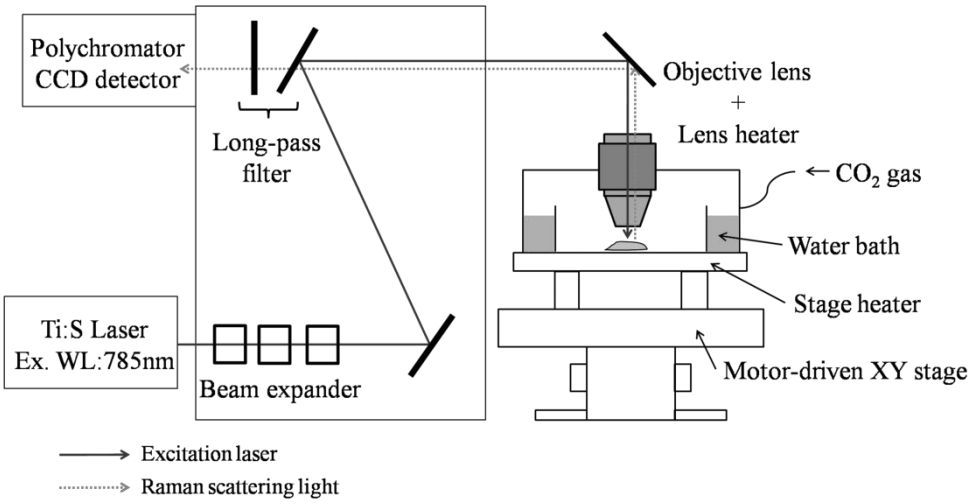

Figure 1

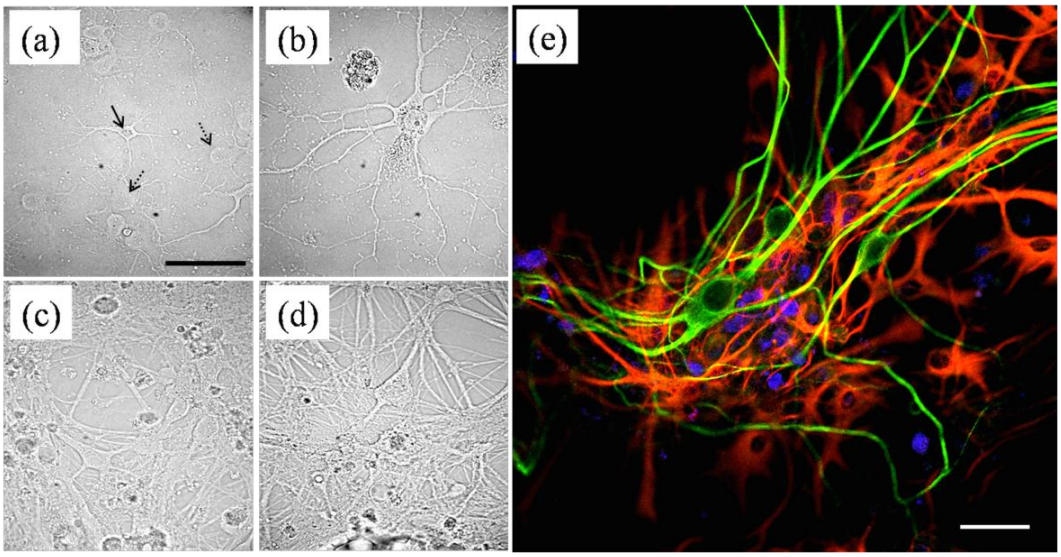

Figure 2

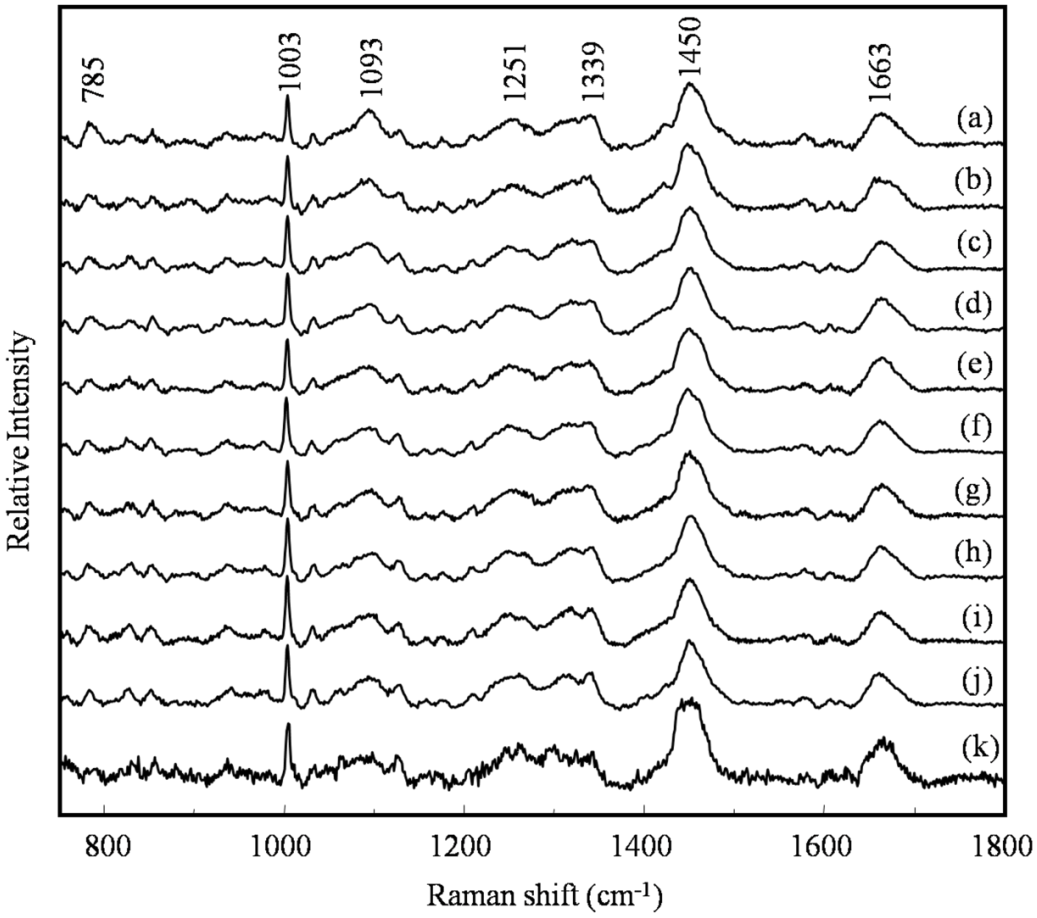

Figure 3

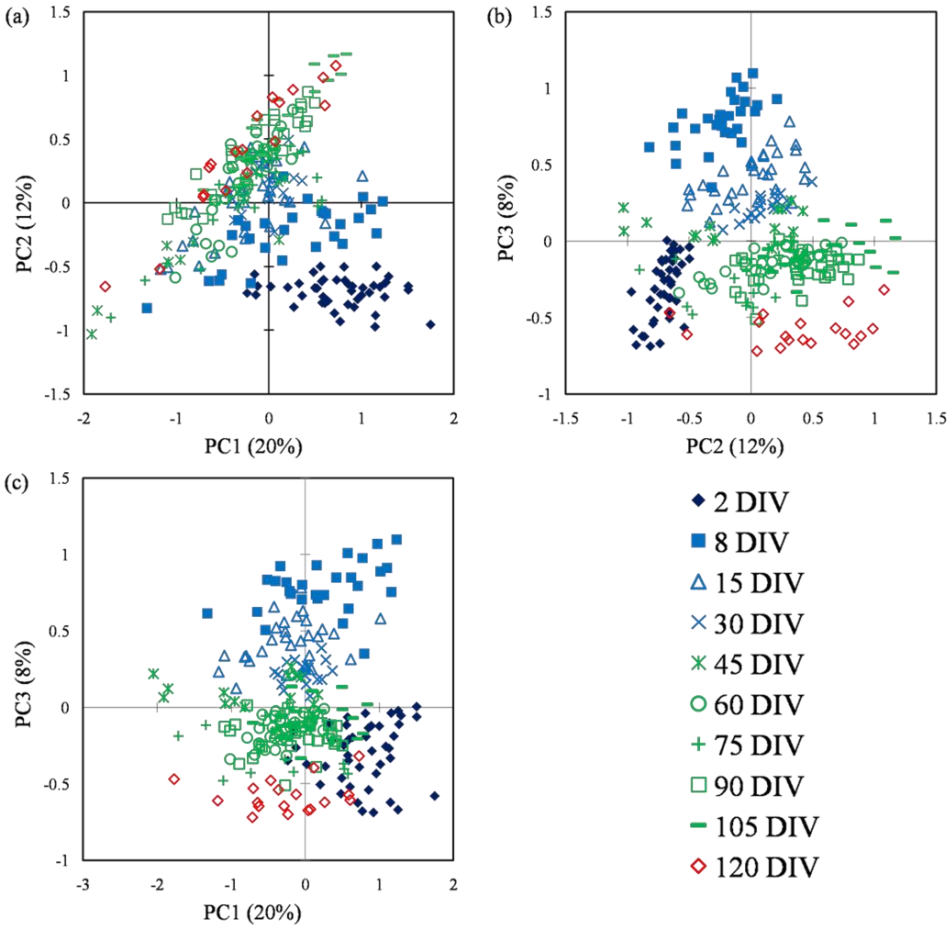

Figure 4

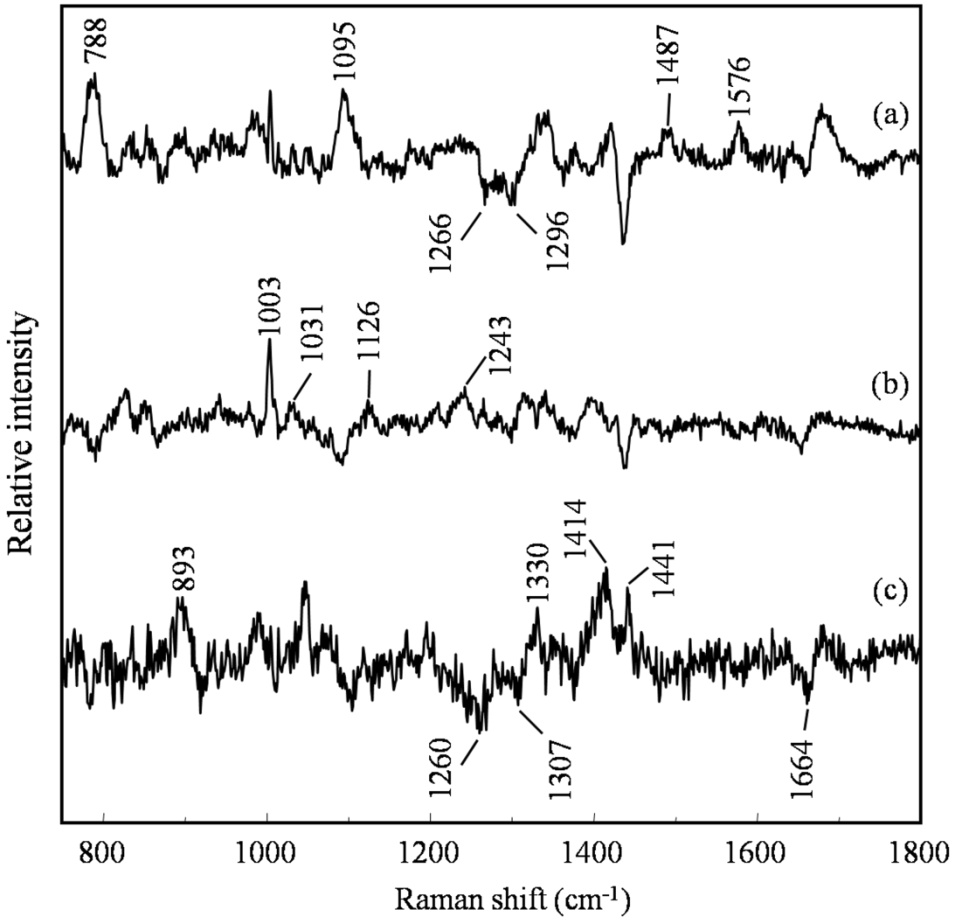

Figure 5